Asphalt Paving Technologists, Vol. 47, 1978, pp. 160-189.
24. P.J. Van de Loo. The Creep Test: A Key Tool in Asphalt Mix Evaluation and in the Prediction of Pavement Rutting. Proc., Assn. of Asphalt Paving Technologists, Vol. 47, 1978, pp. 552-557.

Discussion

David G. Tunnicliff

The authors have presented an interesting and stimulating approach to the use of sand-asphalt base courses. The data in the paper are conclusive and show that the methodology is satisfactory; however, the mixture of Yuma sand and 14 percent asphalt (12.3 percent by weight of mixture) raises questions. Such a high asphalt content in any practical paving mixture is unheard of. If the best asphalt content for this sand-asphalt base mixture is 12.3 percent, the mixture will almost certainly rut excessively and should not be used. Because all of the data are obtained from what appears to be a useless mixture, it is suggested that a practical sand-asphalt mixture be included in future research before it is concluded that the methodology is satisfactory.

Authors' Closure

In response to Tunnicliff's discussion, we believe the methodology is applicable to any asphaltic mixture in view of the similarity between the results we obtained and those obtained by Hofstra and Klomp (5) from a test road and results obtained by Morris (6).

The paper is concerned principally with the properties of a dune-sand paving mixture. We do not believe the material described to be entirely useless. We believe it could be used as a base course for a low-volume road with load restrictions during hot periods, especially in locales that do not have good paving aggregates.

Publication of this paper sponsored by Committee on Characteristics of Bituminous Paving Mixtures to Meet Structural Requirements.

Visco-Elasto-Plastic Constitutive Law for a Bituminous Mixture Under Repeated Loading

MORDECHAI PERL, JACOB UZAN, AND ARIEH SIDES

A constitutive law for a bituminous mixture subjected to repeated loading is presented. The elastic, plastic, viscoelastic, and viscoplastic strain components are incorporated into the model as they are simultaneously present in the loading process. The model parameters are extracted from a series of repeated uniaxial creep and creep recovery experiments conducted under constant compression stress. The experiments were performed at constant temperature for various stress levels, time periods, and numbers of cycles. The elastic strain is found to depend solely and linearly on the stress. The plastic strain is linearly proportional to stress and exhibits a power-law dependence on the number of loading cycles. The viscoelastic strain is nonlinear with respect to stress and is governed by a power law of time. The viscoplastic strain component is nonlinear with respect to stress and thus can be represented by the product of a second-order polynomial of stress and two power laws of time and number of cycles, respectively. The reliability of this constitutive equation was evaluated by means of two verification tests. Good agreement was found between the predicted and measured strains.

In recent years, efforts have been made to develop rational methods for the design of flexible pavements that make it possible to predict pavement performance in terms of fatigue crack growth and rutting. Because the bituminous mixture plays a major role in pavement design, it is imperative to characterize it by a constitutive law that will account for the various effects occurring in in situ service. This constitutive law can be expressed as follows:

$$\epsilon_{ij} = \epsilon_{ij}(\sigma_{ij}, t, N, T) \quad (1)$$

where

ϵ_{ij} and σ_{ij} = strain and stress tensor components, respectively;
t = time;
N = number of loading cycles; and
T = temperature.

N is included in Equation 1 to represent the repetitive loading mode.

In the various approaches to analyzing failure of flexible pavements due to fatigue, the bituminous mixture is assumed to be either a linear (1-3) or a viscoelastic material (4). These models, however, do not fully account for the actual behavior of the bituminous mixture. The effects of factors such as rest period (5,6), healing time (7), and crack retardation, which might increase pavement fatigue life by more than one order of magnitude, cannot be anticipated. Thus, the development of a more rational model for predicting pavement fatigue life under cyclic loading requires a more comprehensive and more realistic material law.

It is the purpose of this paper to present an improved rheological model for the bituminous mixture that accounts for the elastic, plastic, viscoelastic, and viscoplastic responses of the material.

MATERIAL AND SPECIMENS

A single sand-asphalt mixture was used. It con-

tained dolomite aggregate (all of which passes the No. 10 sieve) bound with bitumen of 60-70 penetration grade. The bitumen, aggregate, and mixture properties are given in the following tables. The first table gives properties of the 60-70 grade asphalt, the second table gives properties of the dolomite aggregate, and the third and fourth tables give the gradation data and properties of the sand-asphalt mixture.

Properties of 60-70 grade asphalt

Property	Test Value
Softening point, ring and ball (°C)	54
Penetration at 25°C (0.1 mm)	60-70
Penetration index	+0.3
Ductility at 25°C (cm)	>100
Specific gravity	1.02
Kinematic viscosity at	
50°C	3500
71.1°C	300

Properties of dolomite aggregate

Property	Test Value
Specific gravity	
Material retained on No. 4 sieve	
Bulk	2.70
Apparent	2.76
Material passing No. 4 sieve	
Bulk	2.73
Apparent	2.85
Water absorption (%)	0.9
Los Angeles abrasion test (%)	19-22
Crushing value, British standard (%)	16
Elongation, British standard (%)	9-19
Flakiness, British standard (%)	21-24

Gradation data for sand-asphalt mixture

Sieve Size (mm)	Percentage Passing
2	100
0.84	75
0.425	55
0.18	35
0.074	15

Properties of sand-asphalt mixture

Property	Value
Optimum bitumen content (%)	8.5
Mixture density (kg/m^3)	2300
Marshall stability (lb)	1950
Resilient modulus (MPa)	1395
Marshall flow (0.01 in)	16
Air voids (%)	4.7
Saturation (%)	79.1
Voids in mineral aggregate (%)	22.3

The optimal bitumen content and the mixture density are based on a preliminary Marshall system that complies with ASTM standard D1559.

All of the test specimens used in this study consisted of compressed cylinders 50.8 mm in diameter and 101.6 mm in length made from the above mixture. The specimens were compacted by a vibratory compactor. Careful control was imposed on specimen density. Specimens whose density deviated by more than 0.5 percent from the mean were excluded from the experiments.

EXPERIMENTAL APPARATUS AND PROCEDURE

The time-dependent properties of the sand-asphalt mixture were investigated in a series of repeated uniaxial creep and creep recovery tests. Each loading cycle consisted of two equal periods. During the first period there was specimen creep under constant compression stress, at the end of which the load was removed. Creep recovery followed throughout the second period.

A general view of the experimental setup is shown in Figure 1. A selected deadweight, placed on the loading level, produces a constant load that is transferred to the specimen by a load cell. The uniaxial deformation and the applied load are automatically recorded. The deformation is measured by using a deformation gauge and the applied load by means of the load cell. All outputs are recorded, as a function of time, on both an X-Y recorder and a strip-chart visicorder. The experiments are carried out at a constant temperature of 25° ± 0.5°C. The specimen is immersed in a temperature-controlled water tank for 2.5 hr before the test. It is then transferred to the test cell, within which temperature is further controlled by water circulation.

RESULTS AND ANALYSIS

Two sets of tests were conducted in order to characterize the sand-asphalt mixture. In set 1, the specimens underwent four loading cycles. Each cycle consisted of 1 hr of creep under constant stress followed by 1 hr of creep recovery. In set 2, 20 loading cycles were applied with creep and creep recovery periods of 1 min each. Both sets of tests were performed at four stress levels: 0.1, 0.2, 0.4, and 0.8 MPa. Each of the tests was repeated at least twice to increase the reliability of the results.

Creep and recovery curves for the axial strain during the first loading cycle of test set 1 are shown in Figure 2. These results together with all the other experimental observations suggest that the total strain (ε_t) has recoverable and irrecover-

Figure 1. Experimental setup.

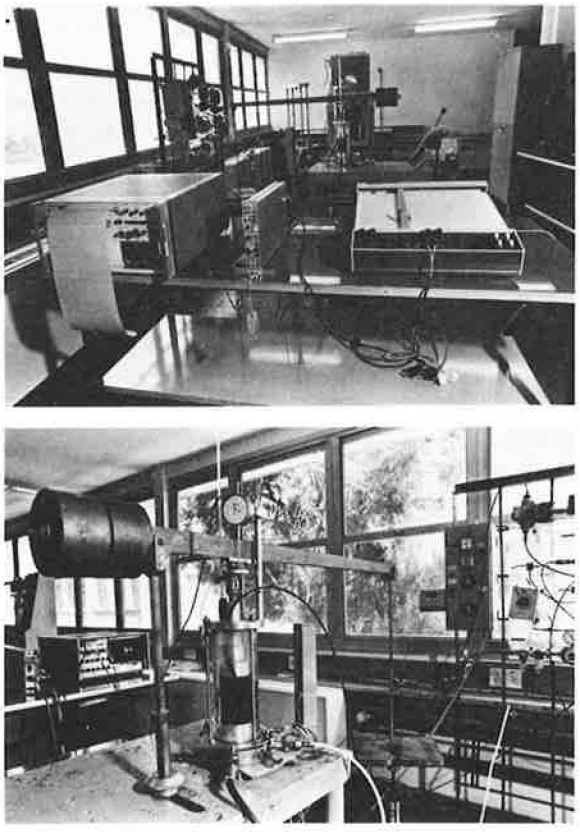

Figure 2. First cycle of creep and recovery curves of test set 1.

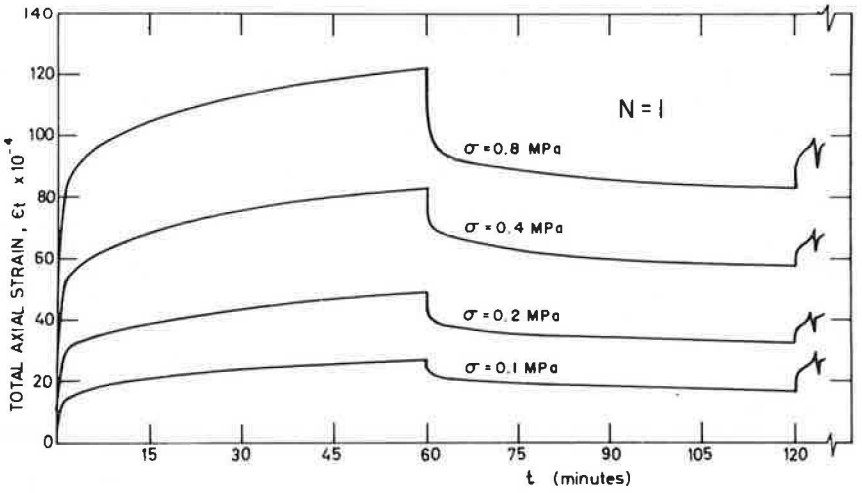

Figure 3. Schematic representation of strain components.

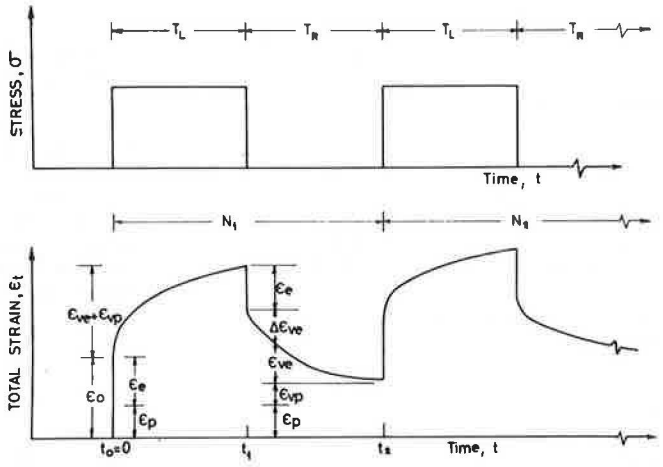

able elements, some of which are time-dependent and some time-independent. Therefore, the total strain can be resolved into four components:

$$\epsilon_t = \epsilon_e + \epsilon_p + \epsilon_{ve} + \epsilon_{vp} \quad (2)$$

where

ϵ_e = elastic strain (recoverable and time independent),
ϵ_p = plastic strain (irrecoverable and time independent),
ϵ_{ve} = viscoelastic strain (recoverable and time dependent), and
ϵ_{vp} = viscoplastic strain (irrecoverable and time dependent).

In a typical schematic cycle (see Figure 3), it can be observed that at $t = t_0$, when load is applied, a strain, ϵ_0, containing the elastic and plastic components, appears instantaneously. As the specimen undergoes creep ($t_0 \leq t \leq t_1$), viscoelastic and viscoplastic strains are built up. Once the load is removed ($t = t_1$), the elastic strain vanishes; in the period that follows ($t_1 \leq t \leq t_2$), part of the viscoelastic strain is recovered. At the end of the cycle the residual strain consists of the irrecoverable plastic and viscoplastic strain components and of the remainder of the viscoelastic strain that has not been recovered.

A detailed analysis of each of the strain components and their dependence on stress level, time, and number of loading cycles is presented below.

Elastic Strain

The elastic strain is obtained from the recovery curves. It is equal to the instantaneous decrease in the total strain that occurs at the moment the load is removed ($t = t_1$ in Figure 3). The elastic strain, evaluated for each cycle of all tests in sets 1 and 2, is shown in Figure 4 as a function of stress. The elastic strain was found to be a linear function of stress with a module of E = 613 MPa and independent of the number of loading cycles.

Plastic Strain

The plastic strain component is evaluated from the creep curve. As previously described (Figure 3), once the specimen is loaded, a strain ϵ_0 appears, consisting of the elastic and plastic strains. Therefore, the plastic strain is equal to

$$\epsilon_p = \epsilon_o - \epsilon_e \quad (3)$$

where ϵ_e was previously calculated.

Figure 5 shows the relation between the plastic strain during the first cycle and the stress level. The cumulative plastic strain versus the number of repetitions N is shown in Figure 6. Both figures

Figure 4. Axial elastic strain versus stress.

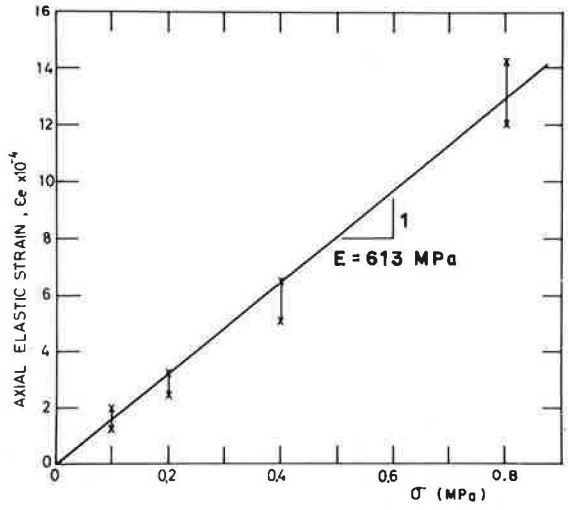

Figure 5. Axial plastic strain versus stress for N = 1.

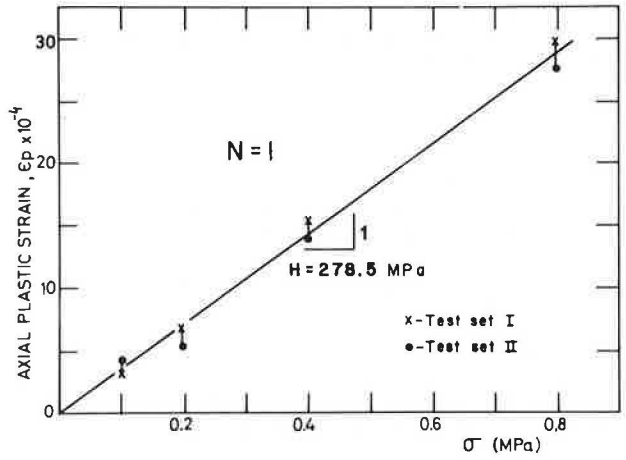

Figure 6. Cumulative plastic strain versus number of cycles.

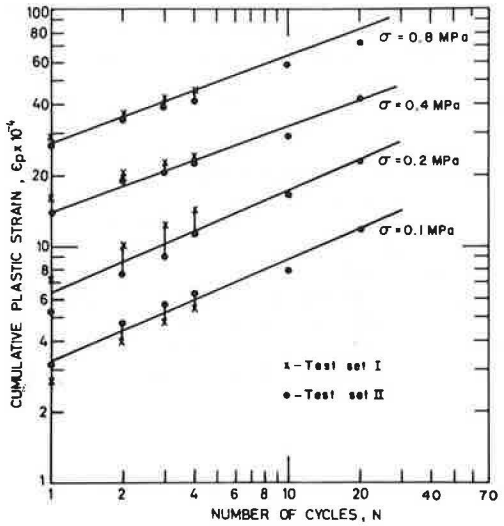

include information from the two sets of tests. The plastic strain in the first cycle (Figure 5) is a linear function of the stress with a mean slope of H = 278.5 MPa. Because plastic deformation appears even under small stresses, it can be assumed that the yield stress is zero for all practical purposes. The variation of the total plastic strain with the number of cycles (Figure 6) is linear, on a log-log scale, with almost the same slope for all stress levels. These observations yield the following expression for the plastic strain:

$$\epsilon_p = (\sigma/H) \cdot N^a \tag{4}$$

where a = 0.35 is obtained by a least-squares fit [the parameter, a, plays a role somewhat similar to that of S, which is used in the context of rutting evaluation (8-10) and whose values are S = 0.1 - 0.44].

Viscoelastic Strain

A detailed analysis of the experimental findings reveals a nonlinear dependence of the viscoelastic strain on time and stress level. The viscoelastic strain is found to be independent of the number of loading cycles. It may be assumed that no creep limit exists because the material undergoes considerable creep even under small stresses. Thus, to determine the recoverable part of the time-dependent strain, the viscoelastic strain component is represented by a product of a power function of time and a function of stress:

$$\epsilon_{ve}(\sigma, t) = A(\sigma)t^{\alpha} \qquad t_1 \geq t \geq t_0 \tag{5}$$

Equation 5 is applicable only to the loading period of the first cycle (Figure 3). Once the load is removed, the viscoelastic strain can be evaluated by using the modified superposition principle (11-14):

$$\epsilon_{ve}(\sigma, t) = A(\sigma)[t^{\alpha} - (t - t_1)^{\alpha}] \qquad t_2 \geq t \geq t_1 \tag{6}$$

The value of α and the function $A(\sigma)$ are obtained from the creep recovery curves. The momentary recovered part of the viscoelastic strain $\Delta\epsilon_{ve}$ (Figure 3) is given by

$$\Delta\epsilon_{ve}(\sigma, t) = \epsilon_{ve}(\sigma, t_1) - \epsilon_{ve}(\sigma, t) \qquad t_2 \geq t \geq t_1 \tag{7}$$

Substituting Equations 5 and 6 into Equation 7 yields

$$\Delta\epsilon_{ve}(\sigma, t) = A(\sigma)[t_1^{\alpha} - t^{\alpha} + (t - t_1)^{\alpha}] \qquad t_2 \geq t \geq t_1 \tag{8}$$

where t is given in seconds, or

$$\Delta\epsilon_{ve}(\sigma, t) = A(\sigma)\psi(t, t_1) \tag{9}$$

A least-squares fit to Equation 9 of all available recovery curves for both sets of tests yields a value of α = 0.29. $A(\sigma)$ is approximated by a procedure similar to a second-order polynomial of the stress (see Figure 7):

$$A(\sigma) = a_1\sigma + a_2\sigma^2 \tag{10}$$

where $a_1 = 8.9 \times 10^{-4}$, $a_2 = -5.0 \times 10^{-4}$, and σ is given in megapascals.

It is worth noting that the viscoelastic strain accumulated during the loading period (T_L) is not completely recovered during the creep recovery phase (T_R) (see Equation 6). Therefore, in the case of repeated loading, a residual viscoelastic strain is built up, the amount of which depends on the ratio (T_R/T_L) and on α. When $T_R = T_L$ (as in test sets 1 and 2), the application of the modified

Figure 7. Function A(σ).

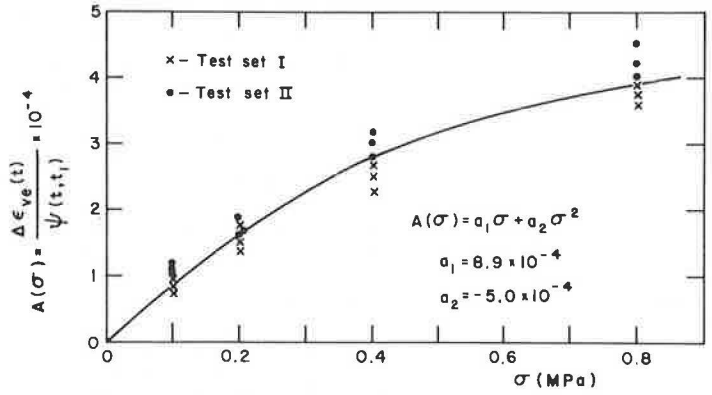

superposition principle results in the following expressions for the viscoelastic strain during the Nth loading cycle and the Nth recovery period, respectively:

$$\epsilon_{ve}(\sigma, t) = A(\sigma)\left\{\sum_{i=1}^{N}[t - (2i-2)T_L]^{\alpha} - \sum_{i=1}^{N-1}[t - (2i-1)T_L]^{\alpha}\right\} \quad (11)$$

$$\epsilon_{ve}(\sigma, t) = A(\sigma)\left\{\sum_{i=1}^{N}[t - (2i-2)T_L]^{\alpha} - [t - (2i-1)T_L]^{\alpha}\right\} \quad (12)$$

Hence, the viscoelastic residual strain at the end of N loading cycles can be shown to be

$$(\Delta\epsilon_{ve})_N = C(N)A(\sigma)T_L^{\alpha}N^{\alpha} = C(N)A(\sigma)t^{\alpha} \quad (13)$$

where C(N) is a weak function of N. For large N, which are of importance in fatigue problems, C is practically a constant.

The last expression in Equation 13 shows that the residual viscoelastic strain depends on the total effective duration of loading ($N \cdot T_L$) rather than on the total number of repetitions (N).

Viscoplastic Strain

The viscoplastic strain component is obtained by subtracting all the previously evaluated strains from the total strain (Figure 3):

$$\epsilon_{vp}(\sigma, t, N) = \epsilon_t(\sigma, t, N) - \epsilon_e(\sigma) - \epsilon_p(\sigma, N) - \epsilon_{ve}(\sigma, t) \quad (14)$$

The experimental data point to the fact that the viscoplastic strain is a function of time, stress level, and number of cycles. Viscoplastic strain occurs even for small stresses. Therefore, it is assumed that no yield or creep limit exists for this strain component.

The viscoplastic strain versus time on a log-log scale for various stress levels, during the first cycle, is shown in Figure 8. Because all lines in Figure 8 exhibit similar slopes, it can be concluded that ϵ_{vp} is proportional to t^{β}. Therefore, ϵ_{vp} during the first loading cycle can be expressed as follows:

$$\epsilon_{vp}(\sigma, t, N = 1) = B(\sigma)t^{\beta} \qquad t_1 \geq t \geq t_0 \quad (15)$$

$$\epsilon_{vp}(\sigma, t, N = 1) = B(\sigma)T_L^{\beta} \qquad t_2 \geq t \geq t_1 \quad (16)$$

where T_L is the loading period and $\beta = 0.22$ (from Figure 8). $B(\sigma)$ is approximated (see Figure 9) by a second-order polynomial of the stress σ:

$$B(\sigma) = b_1\sigma + b_2\sigma^2 \quad (17)$$

where $b_1 = 1.9 \times 10^{-3}$, $b_2 = -8.4 \times 10^{-4}$, and σ is given in megapascals.

Because the viscoplastic strain is irrecoverable, it accumulates as the number of loading cycles increases. In order to quantify this relation, the total viscoplastic strain versus N is plotted in Figure 10 on a log-log scale. The viscoplastic strain at the end of the Nth loading period can thus be stated as

$$\epsilon_{vp}(\sigma, T_L, N) = B(\sigma)T_L^{\beta}N^{b} \quad (18)$$

where b is numerically evaluated from Figure 10 to be b = 0.19. During the Nth loading period, the viscoplastic strain is equal to

$$\epsilon_{vp}(\sigma, t_n, N) = \epsilon_{vp}(\sigma, T_L, N-1) + \Delta\epsilon_{vp}(t_n, N)$$
$$= B(\sigma)T_L^{\beta}(N-1)^{b}[1 + (t_n/T_L)^{\beta}(b/N - b)] \quad (19)$$

where t_n is the time elapsing from the beginning of the Nth cycle. It can be easily shown that Equation 19 reduces to Equation 18 for $t_n = T_L$.

To conclude, the total strain that the sand-asphalt mixture undergoes when subjected to repeated uniaxial loading is given by

$$\epsilon_t(\sigma, t, N) = \epsilon_e(\sigma) + \epsilon_p(\sigma, N) + \epsilon_{ve}(\sigma, t) + \epsilon_{vp}(\sigma, t, N) \quad (20)$$

The detailed expressions for each of the strain components are summarized in Table 1.

Experimental Verification of the Constitutive Law

With the aim of evaluating the accuracy and the reliability of this model in predicting the behavior of the given material, two verification experiments were performed. The first test was carried out at a stress level of $\sigma = 0.3$ MPa with a loading period of $T_L = 10$ sec and a recovery period of $T_R = 60$ sec and consisted of N = 100 cycles. The second test was performed at a stress level of $\sigma = 0.6$ MPa with equal loading and recovery periods of $T_L = T_R = 10$ sec and was repeated for N = 20 cycles.

The values of the parameters for the two tests are chosen to be different from those in test sets 1 and 2 and more similar to those prevailing in situ.

A comparison between the experimentally measured strain and the predicted strain for the first and last cycles of the two tests (N = 1, N = 100 and N = 1, N = 20) is shown in Figures 11 and 12. The results show satisfactory agreement between the measured and predicted values and a maximum deviation of about 14 percent.

CONCLUSIONS

A constitutive law for sand-asphalt mixture subjected to repeated uniaxial loading has been pre-

Figure 8. Axial viscoplastic strain versus time for N = 1.

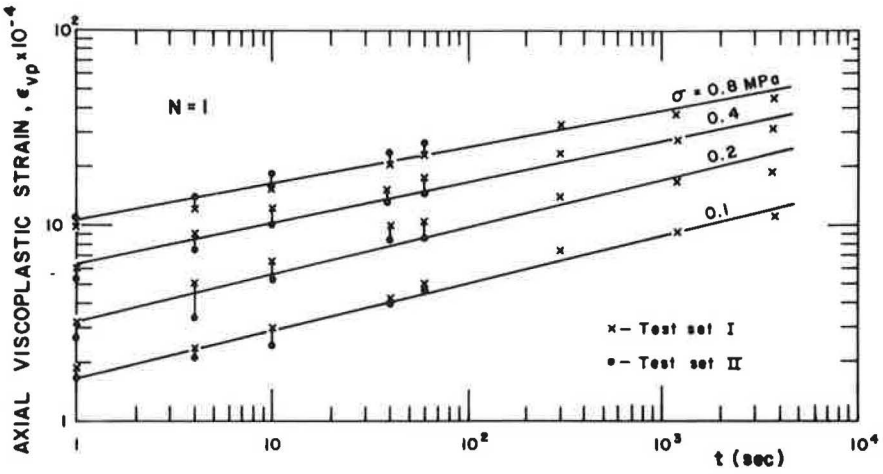

Figure 9. Function B(σ).

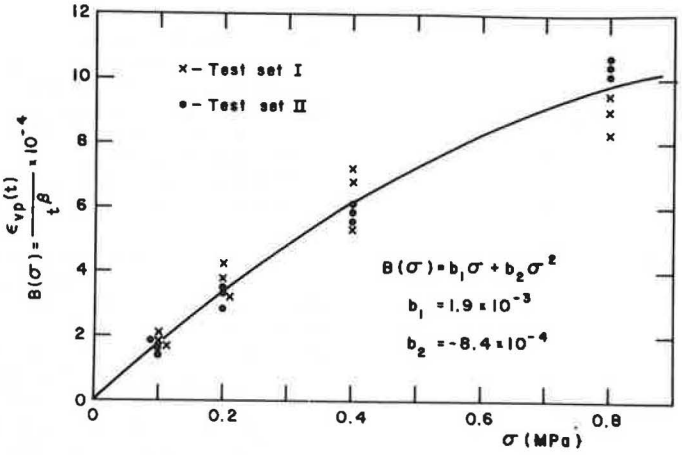

Figure 10. Cumulative viscoplastic strain versus number of cycles.

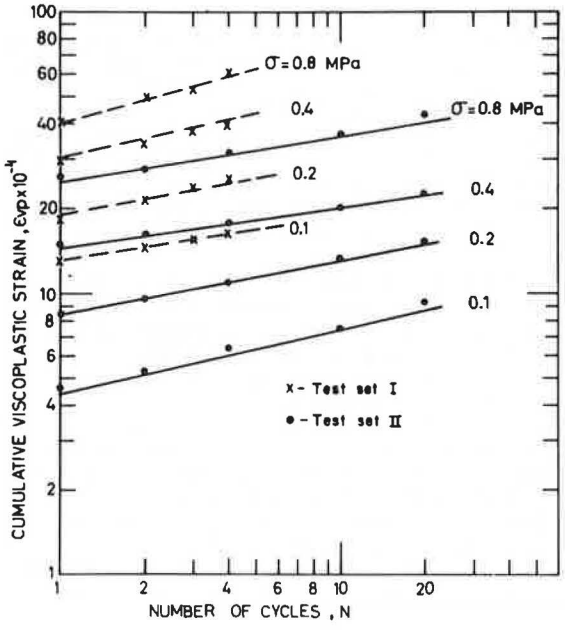

sented. It is shown that the total strain can be separated into four components: elastic, plastic, viscoelastic, and viscoplastic. The explicit dependence of the strain components on stress level, time, and number of repetitions was analyzed. The various parameters of the model were evaluated at a constant temperature of 25°C. The same procedure is applicable to any other temperature as well.

Because the material undergoes plastic, viscoelastic, and viscoplastic strains even at low stress levels, it can be assumed that the yield or creep limit stresses for the above components are practically nonexistent.

From Figures 7 and 9 it is evident that for stresses of less than 0.4 MPa, the viscoelastic and viscoplastic strain components are linear with stress. By means of this information and the fact that the elastic and plastic strains are linearly dependent on stress, can be concluded that for the above range of stress the total strain is a linear function of the stress.

The residual viscoelastic strain given in Equations 12 and 13 might play an important role in fatigue crack growth in pavements. The fatigue crack growth process can be assumed to be controlled by a cumulative strain criterion. Thus, the existence of a residual strain, which on the one hand grows with time (Equation 13) but on the other hand is recover-

Table 1. Strain components.

Cycle	Strain			
	Elastic	Plastic	Viscoelastic	Viscoplastic
First loading period	$\epsilon_e = \sigma/E$, E = 613 MPa	$\epsilon_p = \sigma/H$, H = 278.5 MPa	$\epsilon^a_{ve} = (a_1\sigma + a_2\sigma^2)t^\alpha = A(\sigma)t^\alpha$ $a_1 = 8.9\times10^{-4}$ $a_2 = -5.0\times10^{-4}$, $\alpha = 0.29$	$\epsilon^a_{vp} = (b_1\sigma + b_2\sigma^2)t^\beta = B(\sigma)t^\beta$ $b_1 = 1.9\times10^{-3}$ $b_2 = -8.4\times10^{-4}$, $\beta = 0.22$
First recovery period	-	$\epsilon_p = \sigma/H$	$\epsilon_{ve} = A(\sigma)[t^\alpha - (t - t_1)^\alpha]$	$\epsilon_{vp} = B(\sigma)T_L^\beta$
Loading period of Nth cycle	$\epsilon_e = \sigma/E$	$\epsilon_p = (\sigma/H)N^a$, a = 0.35	$\epsilon^b_{ve} = A(\sigma)\left\{\sum_{i=1}^{N}[t - (2i-2)T_L]^\alpha - \sum_{i=1}^{N-1}[t - (2i-1)T_L]^\alpha\right\}$	$\epsilon_{vp} = B(\sigma)T_L^\beta(N-1)^b[1 + (t_n/T_L)^\beta(b/N - b)]$ b = 0.19
Recovery period of Nth cycle	-	$\epsilon_p = (\sigma H)N^a$	$\epsilon^b_{ve} = A(\sigma)\sum_{i=1}^{N}\{[t - (2i-2)T_L]^\alpha - [t - (2i-1)T_L]^\alpha\}$	$\epsilon_{vp} = B(\sigma)T_L^\beta N^b$

[a]Stress to be taken in megapascals and time in seconds. [b]Only when $T_R = T_L$.

Figure 11. Total strain versus time for first verification test.

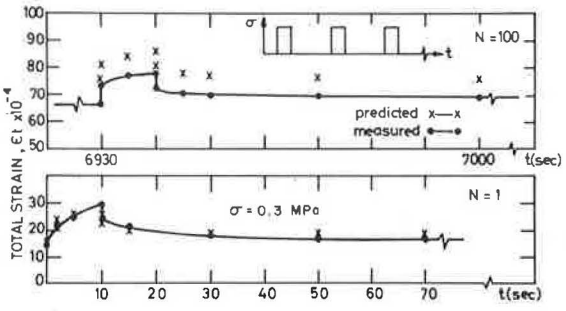

Figure 12. Total strain versus time for second verification test.

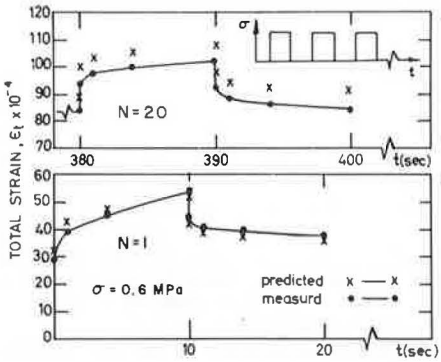

able (provided it is allowed to be so), can explain the phenomena of rest period (5,6) and healing (7).

The model presented in this paper can also be used in predicting pavement rutting, which is an important practical tool in the design of flexible pavements. We are currently examining the subjects of fatigue crack growth and rutting and will subsequently be reporting on the results.

ACKNOWLEDGMENT

The research reported in this paper was supported by the Technion Vice President for Research through L. Deutch Research Fund. We wish to thank Ziss Yehuda for his help with the analysis of the experimental testing data.

REFERENCES

1. C.L. Monismith and others. Asphalt Mixture Behaviour in Repeated Flexture. Institute of Transportation and Traffic Engineering, Univ. of California, Los Angeles, Rept. 70-5, 1970.
2. R.I. Kingham. Failure Criteria Developed from AASHO Road Test Data. Proc., 3rd International Conference on the Structural Design of Asphalt Pavement, London, Vol. 1, Sept. 1972, pp. 656-669.
3. M.W. Witczak. Asphalt Pavement Performance at Baltimore International Airport. Asphalt Institute, College Park, MD, Res. Rept. 4-2, 1974.
4. F. Moavenzadeh, H.K. Findakly, and J.E. Soussou. Synthesis for Rational Design of Flexible Pavements: Volumes 1 and 2. FHWA, Repts. 75-29 and 75-30, 1975.
5. K.D. Raithby and A.D. Sterling. Some Effects of Loading History on the Fatigue Performance of Rolled Asphalts. Transport and Road Research Laboratory, Crowthorne, Berkshire, England, Rept. LR 496, 1972.
6. L. Francken. Fatigue Performance of a Bituminous Road Mix under Realistic Test Conditions. TRB, Transportation Research Record 712, 1979, pp. 30-37.
7. P. Bazin and J.B. Sannier. Deformability Fatigue and Healing Properties of Asphalt Mixes. Proc., 2nd International Conference on the Structural Design of Asphalt Pavements, Univ. of Michigan, Ann Arbor, 1967, pp. 553-569.
8. C.L. Monismith and others. A Subsystem to Predict Rutting in Asphalt Concrete Pavement Structure. Proc., 4th International Conference on the Structural Design of Asphalt Pavements, Univ. of Michigan, Ann Arbor, Vol. 1, 1977, pp. 529-539.
9. B. Rauhut and others. Comparison of Vesys IIM Predictions to Brampton/AASHO Performance Measurements. Proc., 4th International Conference on the Structural Design of Asphalt Pavements, Univ. of Michigan, Ann Arbor, Vol. 1, pp. 131-138, 1977.
10. J. Verstraeten and others. The Belgian Road Research Center's Overall Approach to Asphalt Pavement Structural Design. Proc., 4th International Conference on the Structural Design of Asphalt Pavements, Univ. of Michigan, Ann Arbor, Vol. 1, 1977, pp. 298-324.
11. W.N. Findly and J.S. Lai. A Modified Superposition Principle Applied to Creep Nonlinear

Viscoelastic Materials. Trans., Society of Rheology, Vol. 11, No. 2, 1966, pp. 361-380.
12. J.S. Lai and D. Anderson. Irrecoverable and Recoverable Nonlinear Viscoelastic Properties of Asphalt Concrete. HRB, Highway Research Record 468, 1973, pp. 73-88.
13. W.N. Findly, J.S. Lai, and K. Onaran. Nonlinear Creep and Relaxation of Viscoelastic Materials with an Introduction to Linear Viscoelasticity. North Holland, Amsterdam, 1976.
14. V.W. Cho and W.N. Findly. Creep and Creep Recovery of 304 Stainless Steel Under Combined Stress and Representation by a Viscous Viscoelastic Model. ASME, Journal of Mechanics, No. 80, 1980.

Publication of this paper sponsored by Committee on Characteristics of Bituminous Paving Mixtures to Meet Structural Requirements.

Modification of the Asphalt Institute Bituminous Mix Modulus Predictive Equation

JOHN S. MILLER, JACOB UZAN, AND MATTHEW W. WITCZAK

The dynamic modulus test results for five bituminous mix types (crushed stone, gravel, slag, sand-low P_{200}, sand-high P_{200}) were compared with modulus values predicted by using the Asphalt Institute regression model. Results of this comparison showed an excellent correlation for crushed stone, which was the primary mix type in the model development. For other materials, slag and sand, the results were poor. A correction methodology was developed based on statistical methods to minimize the mean square error between the measured moduli and those predicted by using the model. The model parameter used as the means for correction was the percentage of asphalt content, chosen because it had been shown that the asphalt content range used in model development was narrower than the range encountered in the laboratory study and that, mathematically, it had the greatest effect on the resultant modulus of all the model variables. A unique, material-dependent constant was calculated for each of the five mix types in the study that would be subtracted from the actual asphalt content of the mix for calculating the modulus. A more desirable, generalized method for determining the correction constant was developed based on the difference between the Marshall optimum asphalt content and the actual asphalt content of the mix instead of relying on mix nomenclature (e.g., slag asphalt, sand asphalt). The correction scheme produced a correlation coefficient of 0.891 for all 1179 data points used in this study. This is an excellent result for practical engineering applications.

With the trend toward application of elastic theory to problems in flexible pavement evaluation and design, the development of accurate stress-strain relations for asphalt concrete mixtures is important. Furthermore, asphaltic concrete modulus values have been correlated with substitution ratios or layer coefficients in empirical design methods (1,2) so that an accurate modulus characterization serves both methods. However, direct laboratory modulus characterization under conditions similar to those encountered in the field (dynamic repeated loading, temperature, and load rate) normally requires sophisticated and expensive dynamic laboratory equipment (3). To avoid costly laboratory procedures, alternative methods of determining modulus by using physical and mechanical properties of the mixture were developed. Among these methods were use of the Marshall stability-flow quotient and the development of the Shell nomograph and the Asphalt Institute predictive model.

The Marshall stability-flow quotient was suggested by Nijboer (4) and recommended for use in high temperature ranges by Heukelom and Klomp (5). Nijboer's formula was as follows:

$$S_{60°C,4\ sec} = 1.6\,(\text{stability/flow}) \quad (1)$$

where S is given in kilograms per square centimeter, stability in kilograms, and flow in millimeters. McLeod (6) suggested a variation on the Nijboer formula:

$$\text{Modulus} = 40\,(\text{stability/flow}) \quad (2)$$

where modulus is given in pounds per square inch, stability in pounds, and flow in inches. These formulas use routine laboratory-determined properties of a mix.

The Shell nomograph originally developed by Van der Poel (7) permitted determination of the stiffness of asphalt cement at a particular load rate and temperature as a viscoelastic characteristic as distinguished from elastic modulus. Heukelom and Klomp (5) developed a relation to translate the bitumen stiffness to a mixture stiffness based on volume of aggregate and volume of asphalt cement in the mix. McLeod (6) modified the nomograph by changing the entry temperature criterion. Finally, Claessen and others (8) produced a pair of nomographs to be used together to accomplish the evaluation of bitumen and mixture stiffness used in the current Shell design manual (9).

This paper focuses on the third method for modulus determination, the Asphalt Institute model (10). By examining dynamic modulus values measured in the laboratory for various materials and comparing them with values predicted by the model based on physical properties of the mixture (asphalt content, percentage passing the No. 200 sieve, volume of voids, and asphalt viscosity), the accuracy of the predictor can be established.

RESEARCH PROBLEM STATEMENT

At present, the two predictive models most commonly used are the Shell method and the Asphalt Institute equation. The Shell method is based on stiffness of the asphalt cement determined by entering a nomograph with factors derived from asphalt softening point and penetration and temperature and frequency of loading. This bitumen stiffness is then modified by using a second nomograph to consider volume percentages of aggregate and asphalt cement to give a stiffness or modulus value for the mix.

The Asphalt Institute method was initiated by